Molecular Therapy
Nucleic Acids
Original Article

Regulator of G protein signaling 12 drives inflammatory arthritis by activating synovial fibroblasts through MYCBP2/KIF2A signaling

Gongsheng Yuan,[1] Shu-ting Yang,[1] and Shuying Yang[1,2,3]

[1]Department of Basic and Translational Sciences, School of Dental Medicine, University of Pennsylvania, Philadelphia, PA 19104, USA; [2]The Penn Center for Musculoskeletal Disorders, Perelman School of Medicine, University of Pennsylvania, Philadelphia, PA 19104, USA; [3]Center for Innovation & Precision Dentistry, School of Engineering and Applied Sciences, University of Pennsylvania, Philadelphia, PA 19104, USA

Synovial fibroblasts are the active and aggressive drivers in the progression of arthritis, but the cellular and molecular mechanisms remain unknown. Here, our results showed that regulator of G protein signaling 12 (RGS12) maintained ciliogenesis in synovial fibroblasts, which is critical for the development of inflammatory arthritis. Deletion of RGS12 led to a significant decrease in ciliogenesis, adhesion, migration, and secretion of synovial fibroblasts. Mechanistically, RGS12 overexpression in synovial fibroblasts increased the length and number of cilia but decreased the protein level of kinesin family member 2A (KIF2A). The results of LC-MS analyses showed that RGS12 interacted with MYC binding protein 2 to enhance its ubiquitination activity, through which the KIF2A protein was degraded in synovial fibroblasts. Moreover, overexpression of KIF2A blocked the increases in cilia length and number. Mice with RGS12 deficiency or treatment of RGS12 shRNA nanoparticles significantly decreased the clinical score, paw swelling, synovitis, and cartilage destruction during inflammatory arthritis by inhibiting the activation of synovial fibroblasts. Therefore, this study provides evidence that RGS12 activates synovial fibroblasts' pathological function via promoting MCYBP2-mediated degradation of KIF2A and ciliogenesis. Our data suggest that RGS12 may be a potential drug target for the treatment of inflammatory arthritis.

INTRODUCTION

Inflammatory arthritis is characterized by synovial hyperplasia, articular inflammation, and invasion of the synovium into the adjacent cartilage and bone.[1] Numerous different cells, including synovial fibroblasts, macrophages, B lymphocytes, T lymphocytes, chondrocytes, and osteoclasts, contribute to the destructive process of arthritis.[2] Accumulated studies indicate that activated synovial fibroblasts are one of the most important players in the development of inflammatory arthritis.[3,4] Synovial fibroblasts predominantly contribute to the progression of arthritis by attaching to, invading into, and degrading cartilage and bone.[5–7]

One important characteristic of synovial fibroblasts often noted is the presence of a primary cilium.[8,9] Primary cilia are non-motile and antenna-like structures that play key roles in sensory functions, cell cycle mediation, neurogenesis, and skeletal development.[10] Ciliopathies, rare recessive human disorders, include mental retardation, obesity, and various developmental malformations and are caused by malfunctions in ciliary proteins (e.g., kinesin family member protein 2A [KIF2A]) localized to cilia and ciliary basal bodies.[11,12] Genetic experiments have revealed that cilia are required for mediating inflammatory signaling.[9] Primary cilia have been reported to contribute to interleukin-1β-induced nuclear factor κB signaling by mediating IKK activity and controlling the inflammatory response.[13] However, whether primary cilia involve in the pathogenesis of inflammatory arthritis remains unknown.

Regulator of G protein signaling (RGS) proteins have important functions in innate and adaptive immunity.[14] RGS1 is upregulated in vascular inflammation, which further promotes leukocyte accumulation.[15] Interestingly, RGS21 and RGS18 have been revealed to regulate cilia function,[16] while RGS18 controls the development of cilia in hair cells.[17] As the multifunctional RGS protein, RGS12 is involved in various human diseases, including bone defects and oral cancer, by regulating post-translational modifications such as phosphorylation, ubiquitination, and SUMOylation.[18,19] Functional genomic screen data by Kim et al.[20] showed that RGS12 is a positive regulator of ciliogenesis in human retinal pigmented epithelium cells. However, the function and mechanism of RGS12 in regulating ciliogenesis and immune diseases remain undefined.

In this study, we investigated the critical roles and mechanisms of RGS12 in regulation of cilia, the synovium tissues and synovial fibroblasts by using CAG-CreER; RGS12$^{fl/fl}$ mice. Our data demonstrated that RGS12 plays a critical role in activating synovial fibroblasts by enhancing ciliogenesis, which in turn triggers arthritis.

Received 26 January 2022; accepted 22 December 2022;
https://doi.org/10.1016/j.omtn.2022.12.017.

Correspondence: Shuying Yang, Department of Basic and Translational Sciences, University of Pennsylvania, School of Dental Medicine, 240 S 40th Street, Levy 437, Philadelphia, PA 19104, USA.
E-mail: shuyingy@upenn.edu

RESULTS

RGS12 expression and ciliogenesis are increased in the synovial fibroblasts of inflammatory arthritis mice

The synovium is the primary site of inflammatory arthritis. To determine the biological functions of the synovium in inflammatory arthritis, we created the collagen antibody-induced arthritis (CAIA) mouse models by injecting a specific combination of monoclonal antibodies (mAb cocktail). We found that the CAIA mice demonstrated severe ankle swelling (Figure 1A), swollen synovium, and bone erosion (Figure 1B) by morphological and histological observations. Additionally, the synovitis score and the cartilage destruction score were significantly increased in CAIA mice compared with those in the control mice (Figure 1C). We also found synovitis marker genes including *IL1β*, *IL6*, *MMP1*, and *MMP3* were significantly increased in the synovium of CAIA mice (Figure S1). To determine whether RGS12 in synovial fibroblasts plays a role in inflammatory arthritis, we performed the immunofluorescence in synovial tissues. The results showed that RGS12 is significantly increased in synovium and synovial fibroblasts in CAIA mice (Figure 1D). Interestingly, in the synovium of CAIA mice, we found that the cilia length was significantly increased in synovial fibroblasts (Figure 1E).

Ablation of RGS12 inhibits the development of inflammatory arthritis by prohibiting ciliogenesis and inflammatory cytokines and enzymes in synovial fibroblasts

To determine the functions of RGS12 *in vivo*, we crossed mice with a floxed RGS12 allele with CAG-CreER mice to create the inducible CAG-CreER; $RGS12^{fl/fl}$ (RGS12 knockout [KO]) mice. Cre recombinase expression was induced by tamoxifen to delete the RGS12 gene in mice (Figure 2A). Deficiency of RGS12 in the synovium of RGS12 KO mice was confirmed by immunoblotting after tamoxifen induction for 5 consecutive days (Figure 2B). To determine the role of RGS12 in inflammatory arthritis, we induced the CAIA models in control (CAG-CreER) and RGS12 KO mice by intraperitoneal injection of mAb cocktails on day 0 and sacrificed the mice on day 9 (Figure 2C). The ankles of RGS12 KO mice showed less hypertrophy than control mice with arthritis (Figure 2D). The ankle width and clinical score of RGS12 KO mice were significantly lower than those of control mice with arthritis (Figures 2E and 2F), but the mean weight showed no difference between the two groups (Figure 2G). Moreover, the histological results showed that the synovitis score and cartilage destruction score were decreased in RGS12 KO mice with CAIA (Figure 2H). The IL1β and IL6 protein levels in inflamed synovium were also decreased in RGS12 KO mice with CAIA in comparison with the control group (Figure 2I).

To study the functions of synovial fibroblasts in arthritis, we isolated primary synovial fibroblasts from the ankle synovium of control and RGS12 KO mice with CAIA (Figure 2J). To determine whether RGS12 is a key regulator of cilia, we analyzed the Genome RNAi database (http://www.genomernai.org/v17/genedetails/6002) and found the knockdown of RGS12 resulted in the reduction of cilia length, which suggests that RGS12 is a critical regulator of cilia formation (Table S1). As expected, we found that the loss of RGS12 significantly decreased the cilia lengths and ciliated cell numbers in synovial fibroblasts from RGS12 KO mice with CAIA compared with control mice (Figure 2J). Moreover, the levels of synovitis marker genes, including *IL6*, *IL1β*, *MMP1*, and *MMP3*, were significantly decreased in RGS12 KO mice with CAIA compared with control groups (Figure 2K).

RGS12 regulates the ciliogenesis, migration, attachment, and activation of synovial fibroblasts

To identify the function of RGS12 in synovial fibroblasts, we stably transfected porcine cytomegalovirus (pCMV)-RGS12 plasmids (RGS12 overexpression [RGS12 OE]) into primary synovial fibroblasts. The synovial fibroblasts with deficient RGS12 were harvested from the RGS12 KO mice and confirmed the loss of protein expression by immunoblotting (Figure S2). By analyzing the feature of cilia via immunofluorescence, we found that RGS12 OE increased cilia length, whereas RGS12 KO decreased the cilia length in synovial fibroblasts (Figure 3A). Previous studies showed that cilia mainly affect cell adhesion.[21,22] To further understand whether RGS12 contributes to cell adhesion, which causes the phenotypic abnormalities, a plastic adhesion assay was performed in RGS12 OE and KO synovial fibroblasts. The results showed that synovial fibroblasts with RGS12 OE mostly adhered to tissue culture plastic; however, synovial fibroblasts with RGS12 KO poorly adhered and expanded on tissue culture plates (Figure 3B). Moreover, the flipping assay showed enhanced synovial fibroblasts-chondrocytes adhesion in RGS12 OE group but decreased adhesion with the RGS12-deficient group compared with the control group (Figure 3C). Given that synovial fibroblasts play a role in arthritis pathogenesis through aggressive migration,[23] we examined the migration of synovial fibroblasts using a Boyden chamber assay. As shown in Figure 3D, the number of migrated synovial fibroblasts was increased by approximately 1.9-fold in the RGS12 OE group, but decreased by 46% in the RGS12 KO group compared with the control group. To evaluate cell proliferation, we then performed a WST-1 assay and found that synovial fibroblast proliferation was not significantly changed after RGS12 OE or KO compared with that in control synovial fibroblasts (Figure 3E). Furthermore, we found the levels of the synovial fibroblast markers *IL6*, *IL1β*, *MMP1*, and *MMP3* were increased in RGS12 OE, but slightly decreased without statistical difference in RGS12 KO synovial fibroblasts compared with those in the control group (Figure 3F). Consistently, we also confirmed the functions of RGS12 in human synovial cells (SW982 cells) and found that the RGS12 OE promoted the human synovial fibroblast attachment (Figure S3A), migration (Figure S3B), and activation evidenced by significantly increased *MMP1* and *MMP3* expression (Figure S3D). Moreover, the results from WST-1 assay for cell proliferation analysis showed that RGS12 OE did not affect human synovial cell proliferation (Figure S3C).

RGS12 drives the ciliogenesis by promoting the degradation of KIF2A

Since fibroblasts originate from and share the most features of bone marrow cells,[24,25] we further analyzed the protein profiles from

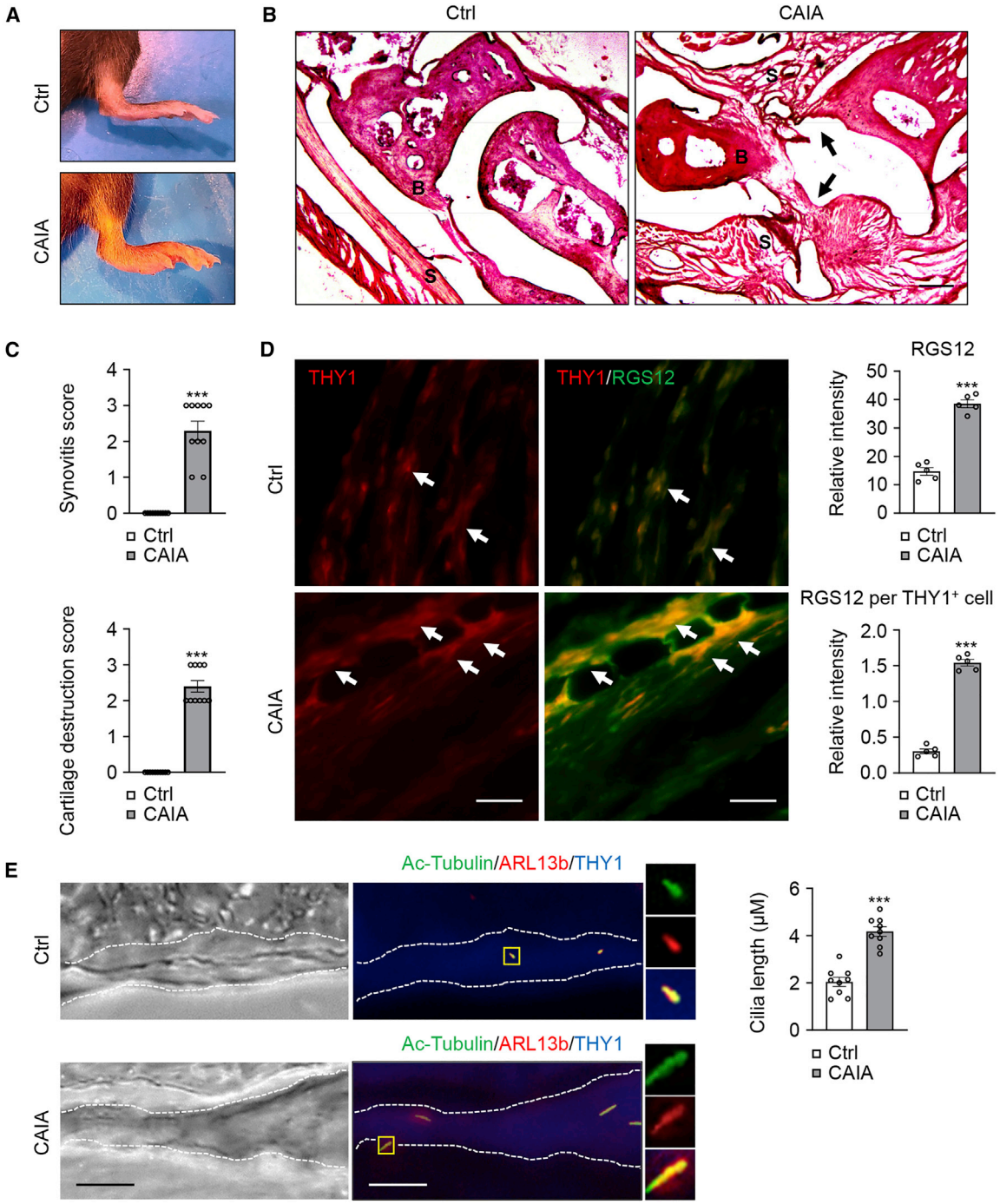

Figure 1. RGS12 expression and ciliogenesis increased in the synovial fibroblasts from inflammatory arthritis mice

(A–C) CAIA mouse models were induced in C57BL/6 mice by injecting 5 mg mAb mixture for 9 days (Chondrex #53100). (A) Photographs of representative hind-paws from the control (Ctrl) and CAIA mouse models. (B) Hematoxylin and eosin staining of synovial tissues from Ctrl and CAIA mice. B, bone area; S, synovium. Scale bar, 200 μm. (C) Synovitis score and cartilage damage score were evaluated in (B). The data are expressed as the means ± standard error of the mean (n = 10; ***$p < 0.001$). (D) THY1 and RGS12 showed colocalization in synovium from the Ctrl and CAIA mice. White arrows indicated the RGS12 in THY1$^+$ cells. Scale bar, 25 μm. The quantitative data of the relative intensity of RGS12 (top) and the relative intensity of RGS12 per THY1$^+$ cell (bottom). The data are expressed as the means ± standard error of the mean (n = 5; ***$p < 0.001$). (E) The primary cilia of synovial fibroblasts from Ctrl and CAIA mice were stained by immunofluorescent assay (green, Ac-Tubulin; red, ARL13b; blue, THY1; scale bar, 10 μm). The quantitative data showed the cilia length (n = 10; ***$p < 0.001$).

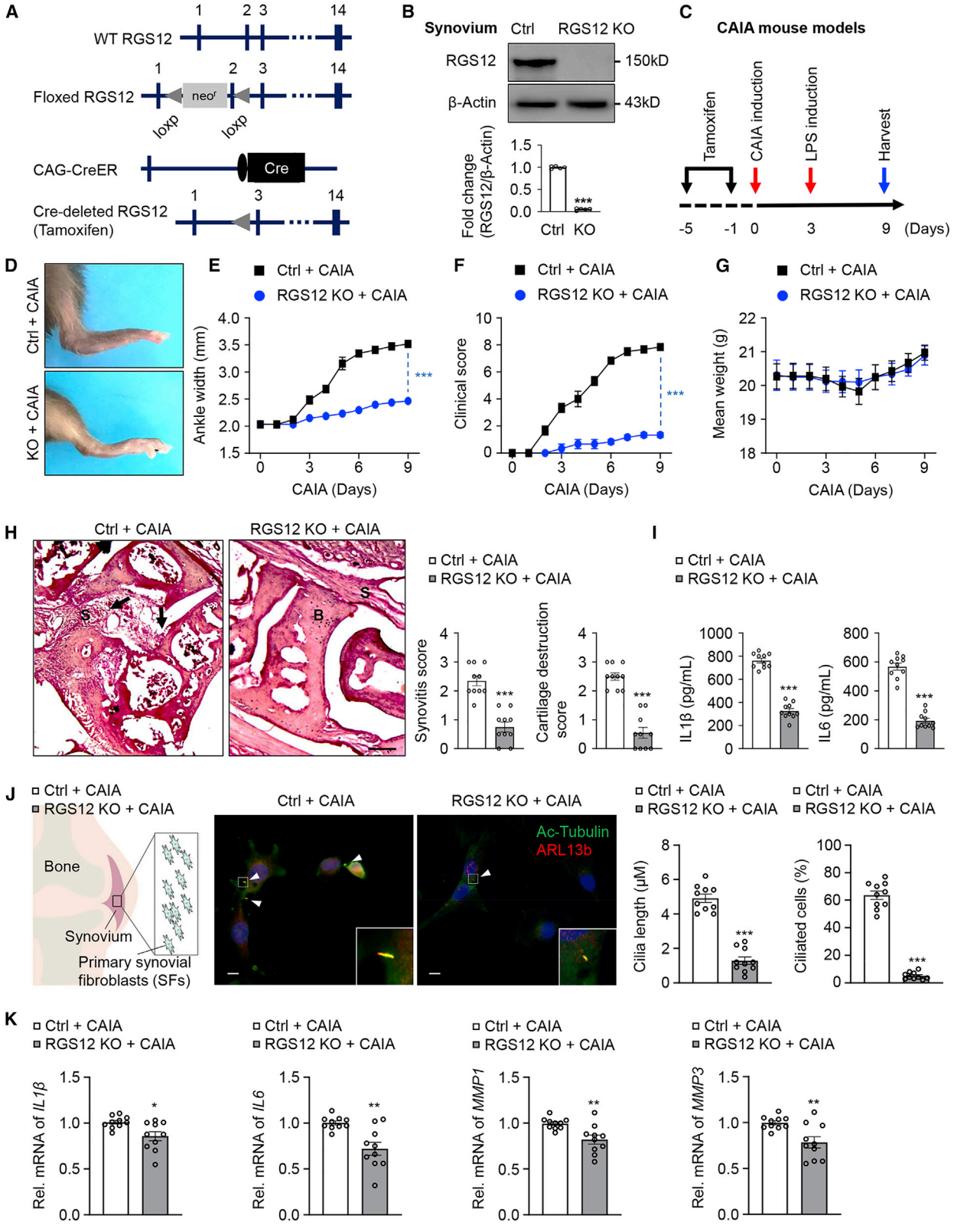

(legend on next page)

control and RGS12 KO bone marrow cells by liquid chromatography/mass spectrometry (LC-MS) and identified the top 5 upregulated and downregulated proteins (Figure 4A). Given that RGS12 plays a critical role in ciliogenesis, we then performed a Venn analysis to identify the overlapping proteins between the LC-MS results and CiliaCarta database (Figure 4B).[26] We discovered the five ciliary proteins with the most significant expression changes and found that KIF2A was the most upregulated protein ($p < 0.05$) after the ablation of RGS12 in bone marrow cells (Figure 4C). To further confirm the role of KIF2A in the regulation of cilia formation in fibroblasts, pCMV-KIF2A was stably transfected into the mouse primary synovial fibroblasts, we found that the forced expression of KIF2A impaired ciliogenesis (Figure S4). To determine the relationship between RGS12 and KIF2A in synovial fibroblasts, we examined the expression of KIF2A by immunoblotting in RGS12 KO and OE synovial fibroblasts. Consistent with the LC-MS data, the KIF2A level was increased in RGS12 KO, but decreased in RGS12 OE synovial fibroblasts (Figure 4D). However, we found RGS12 neither binds to KIF2A nor regulates the transcription levels of KIF2A (Figure S5). Since RGS12 is a critical ubiquitination or SUMOylation regulator when it is activated,[19] we performed co-immunoprecipitation to identify whether RGS12 regulates KIF2A degradation through ubiquitination. Most interestingly, RGS12 OE not only increased the level of ubiquitin (Ub), but also promoted the combination of Ub and KIF2A in synovial fibroblasts (Figure 4E). To further determine whether KIF2A can inhibit ciliogenesis caused by RGS12, RGS12 OE, and KIF2A OE or control plasmids were co-transfected into synovial fibroblasts. We found that the overexpression of KIF2A partially restored the inhibition of ciliogenesis, even in the presence of RGS12 (Figures 4F and 4G).

RGS12 promotes the degradation of KIF2A by enhancing the association of KIF2A-MYCBP2

To gain further insight into the relationship between RGS12 and KIF2A, we performed co-immunoprecipitation to pull down the RGS12 binding proteins and analyzed them by LC-MS (Figure 5A). After performing a Reactome analysis, we confirmed that SUMOylation and ubiquitination signaling play major roles in RGS12 binding proteins (Table S2). These Ub-related proteins were further constructed to an RGS12 interacting protein network by combining with the LC-MS data and Search Tool for the Retrieval of Interacting Genes/Proteins (STRING) database (Figure 5A). We identified the top five Ub-related proteins and found that MYC binding protein 2 (MYCBP2) was the most reliable ligase (with five unique peptides) that binds to RGS12 (Figure 5A).

To further validate the correlations of RGS12 with Ub ligases in fibroblasts, we performed Pearson's correlation analysis by Gene Expression Profiling Interactive Analysis (GEPIA) 2 (Figure 5B). As expected, the RGS12 signature was significantly correlated with the MYCBP2 signature ($R = 0.19$; $p = 0.003$) in fibroblasts but was not correlated with the RING1, RBBP6, HERC2, or LTN1 signature ($p > 0.05$) (Figure S6). Additionally, RGS12 and MYCBP2 showed co-localization in primary synovial fibroblasts by immunofluorescence staining (Figure 5C). We then confirmed through an immunoprecipitation assay that RGS12 interacts with MYCBP2 (Figure 5D). Strikingly, we found that the overexpression of RGS12 significantly enhanced the interaction between MYCBP2 and KIF2A (Figure 5E). Thus, these results suggested that RGS12 promotes the degradation of KIF2A through MYCBP2 in synovial fibroblasts.

Synovial injection of shRGS12 nanoparticles inhibits the progression of inflammatory arthritis by decreasing the ciliogenesis and synovial fibroblast activity

To examine the therapeutic efficacy of decreased RGS12 expression in the joint synovium during the pathogenesis of arthritis, we performed the synovial injection of shRGS12 nanoparticles (NPs) 7 days before the induction of CAIA and administered twice per week for 2 weeks thereafter (Figure 6A). Decreased expression of RGS12 was confirmed in primary synovial fibroblasts by immunoblotting and real-time PCR from the CAIA mice after the injection of shCtrl and shRGS12 NPs into synovium for 2 weeks (Figure S7). Interestingly, we found that, in comparison with shCtrl NPs, synovial injection of shRGS12 NPs decreased the ankle width and the clinical score during arthritis (Figure 6B). Consistent with this result, the swollen synovium, synovitis, and cartilage destruction in CAIA mice were decreased after shRGS12 NPs treatment (Figures 6C and 6D). Moreover, the levels of *IL6*, *IL1β*, *MMP1*, and *MMP3* in the synovium from CAIA mice were decreased

Figure 2. Ablation of RGS12 inhibits the development of inflammatory arthritis by repressing ciliogenesis and inflammatory cytokines/enzymes in synovial fibroblasts

(A) Organization of the wild-type (WT) RGS12 allele, the foxed RGS12 construct, the CAG-CreER transgene, and the recombinant RGS12 allele. Exons were indicated as dark blue boxes. Cre: Cre recombinase coding sequence; *neo*: neomycin resistance gene; and *loxP*: *loxP* sites. (B) Immunoblot analysis of synovium lysates isolated from the ankles showing the absence of RGS12 protein in RGS12 KO mice. (n = 5; ***$p < 0.001$.) (C) Tamoxifen was introduced through the intraperitoneal injection every 24 h for a total of 5 consecutive days before CAIA induction. CAIA was induced in control (Ctrl) and RGS12 KO mice by injection 5 mg of a mAb mixture (Chondrex #53100) suspended in sterile PBS and subsequent challenge with 50 μg lipopolysaccharide on day 3. The mice were sacrificed after immunization on day 9. (D) The ankles of Ctrl and RGS12 KO mice were immunized with the mAb mixture for 9 days. (E–G) Ankle widths (E), clinical scores (F), and mean weight (G) of Ctrl and RGS12 KO mice were evaluated every day for 9 days. The data are expressed as the means ± standard error of the mean (n = 3; ***$p < 0.001$). (H) Hematoxylin and eosin staining of synovial tissues from mice as described in (C). B, bone area; S, synovium. Scale bar, 200 μm. The synovitis score and cartilage destruction score were shown on the right. The data are expressed as the means ± standard error of the mean (n = 10, ***$p < 0.001$). (I) Levels of the IL1β and IL6 in the lysates of synovium isolated from the Ctrl and RGS12 KO mice with CAIA. The data are expressed as the means ± standard error of the mean (n = 10; ***$p < 0.001$). (J) The primary synovial fibroblasts were isolated by magnetic beads assay from the Ctrl and RGS12 KO mice with CAIA induction (9 days). The primary cilia in synovial fibroblasts from Ctrl and RGS12 KO mice with CAIA were stained by immunofluorescent assay (green, Ac-Tubulin; red, ARL13b; scale bar, 10 μm). The lengths of cilia and the ciliated cell numbers were analyzed in (J) (n = 10; ***$p < 0.001$). (K) The relative mRNA levels of *IL1β*, *IL6*, *MMP1*, and *MMP3* in synovial fibroblasts as described in (J) were analyzed. The values are the mean ± standard error of the mean (n = 10; *$p < 0.05$; **$p < 0.01$).

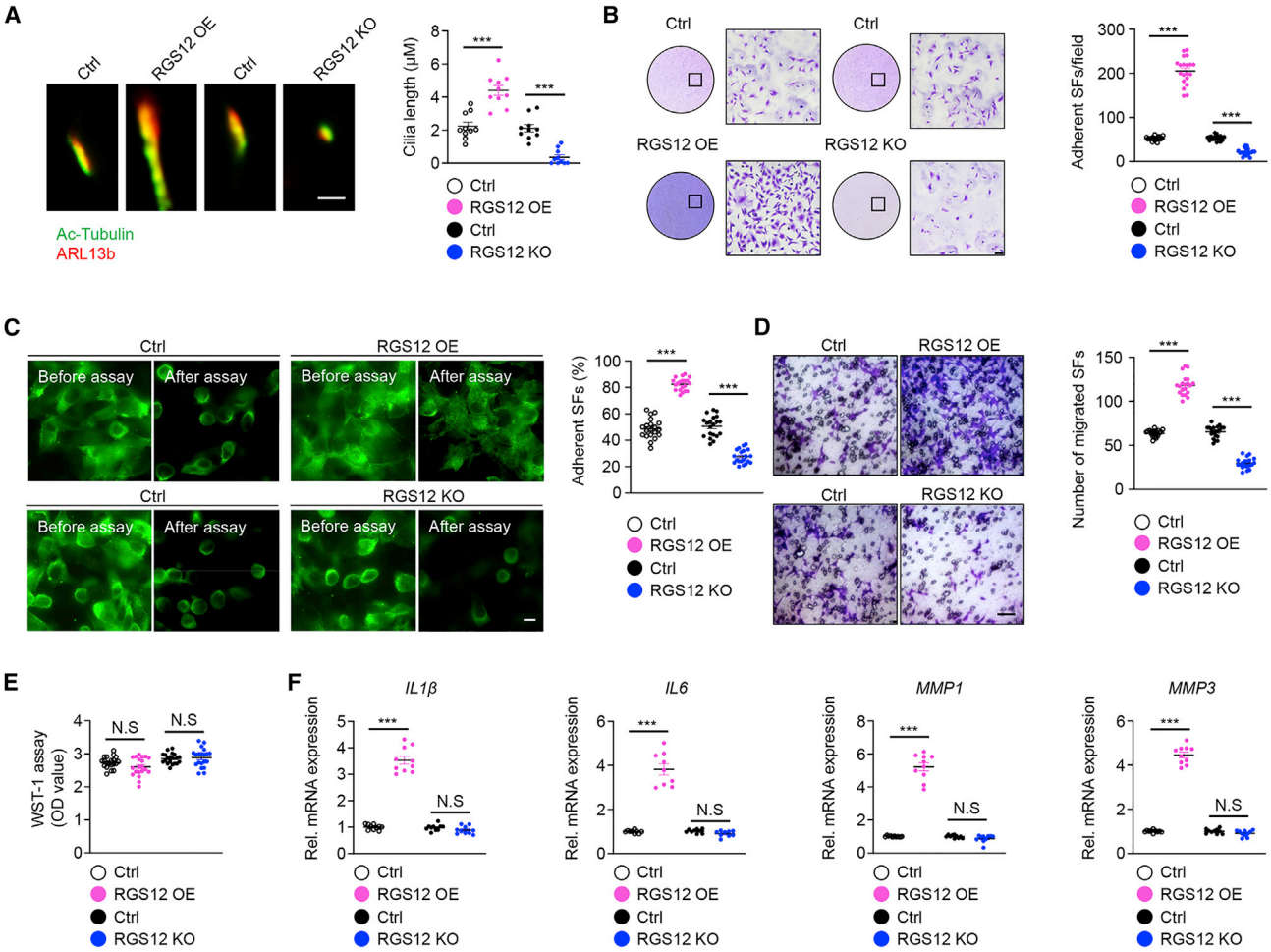

Figure 3. RGS12 regulates the ciliogenesis, migration, attachment, and activation of synovial fibroblasts

(A) The primary synovial fibroblasts were harvested from the control (Ctrl) and RGS12 KO mice. For overexpression of RGS12 (RGS12 OE), the primary synovial fibroblasts from WT Ctrl mice were stably transfected with pCMV-RGS12 plasmids. Immunofluorescent staining of primary cilia in synovial fibroblasts (green, Ac-Tubulin; red, ARL13b; scale bar, 2 μm). The quantitative data showed the cilia length (n = 10; ***$p < 0.001$). (B) Adhesive nature of synovial fibroblasts in culture plastics. Gross (round) and magnified (square) images of culture morphology. Relative statistics are shown on the right (n = 20; ***$p < 0.001$; scale bar, 100 μm). (C) Synovial fibroblasts were stably transfected with pCMV-GFP plasmids. The GFP-labeled synovial fibroblasts were added to confluent chondrocyte layers and incubated for 2 h for flipping assay. The attached synovial fibroblasts (SFs) were counted in five different wells (n = 20; ***$p < 0.001$; scale bar, 10 μm). (D) Measurement of synovial fibroblast migration using a transwell system. Migrated synovial fibroblasts were photographed and counted (n = 20; ***$p < 0.001$; scale bar, 200 μm). (E) Synovial fibroblast proliferation was measured by the WST-1 colorimetric assay (N.S., not significant; n = 20). (F) The relative mRNA expression levels of *IL1β*, *IL6*, *MMP1*, and *MMP3* in synovial fibroblasts were evaluated by real-time PCR assay from the Ctrl, RGS12 OE, and RGS12 KO mice. The values are the mean ± standard error of the mean (n = 10; ***$p < 0.001$; N.S., not significant).

after the introduction of shRGS12 NPs in comparison with shCtrl NPs (Figure 6E).

To determine whether shRGS12 NPs affect the fibroblasts in inflammatory arthritis, we harvested the primary synovial fibroblasts from CAIA mice with shCtrl NPs or shRGS12 NPs treatment (Figure 6F). We found that shRGS12 NPs inhibited the migration, adhesion, and ciliogenesis of synovial fibroblasts in inflammatory arthritis (Figures 6G–6I). To further confirm whether shRGS12 NPs inhibit synovitis by inhibiting the degradation of KIF2A, immunoblotting was performed in synovial fibroblasts from CAIA mice with shCtrl or shRGS12 NPs treatment. As expected, the results showed the shRGS12 NPs reduced the Ub levels and increased the KIF2A levels in synovial fibroblasts during inflammatory arthritis (Figure 6J).

DISCUSSION

Synovial fibroblasts are the main stromal cells in the synovium that produce extracellular matrix components and are essential for cartilage integrity and healthy joints.[1,3,27] During the development of arthritis, the synovium thickens, and immune cells infiltrate into the sublining layer of the synovium.[28–30] Synovial fibroblasts are recently regarded as innate immune cells because of their expression

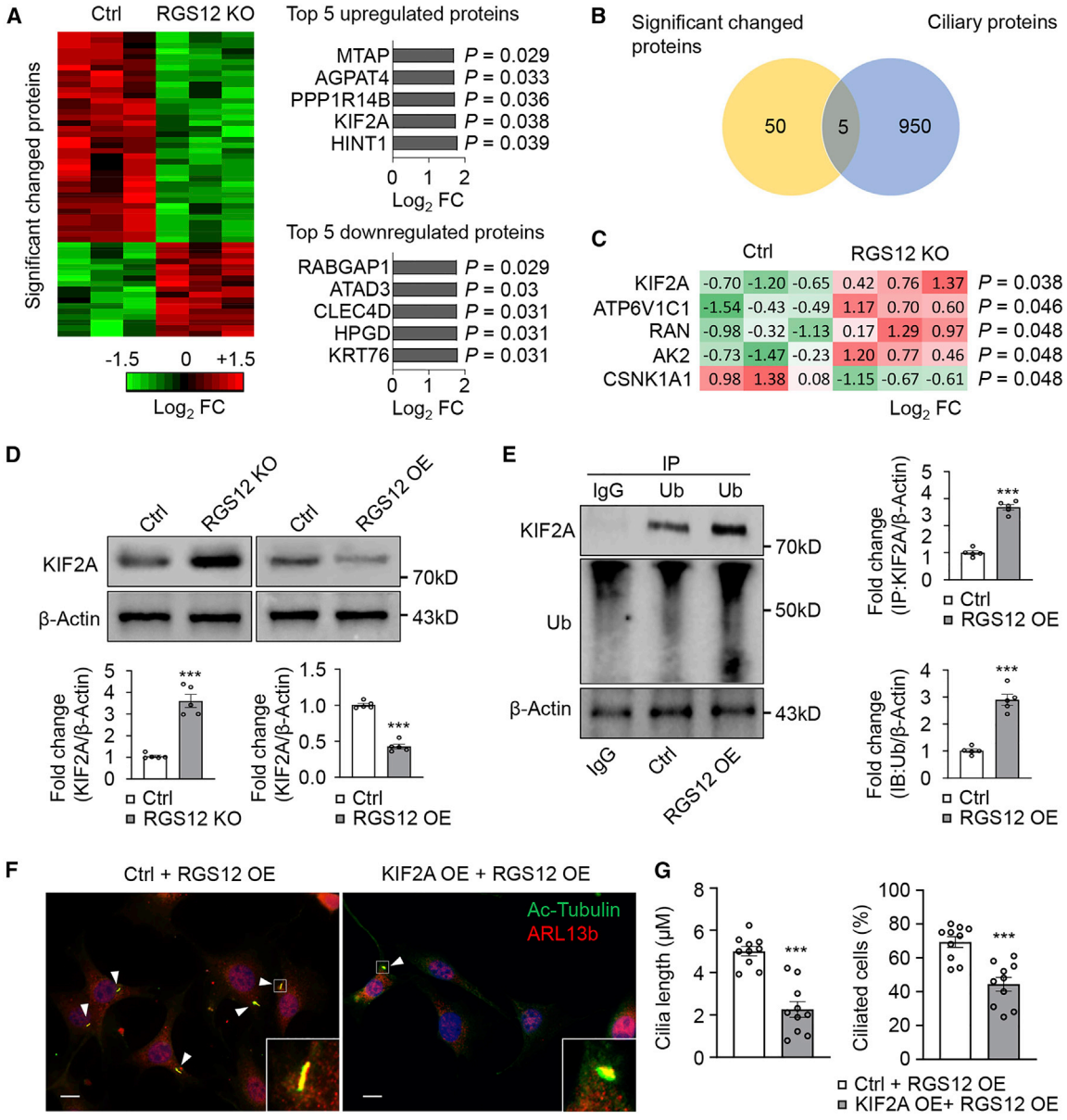

Figure 4. RGS12 drives the ciliogenesis by promoting the degradation of KIF2A

(A) Heatmap depicting the proteins which were up-regulated and down-regulated in RGS12 KO bone marrow cells as compared with control cells (n = 3; $p < 0.05$). The top five upregulated and downregulated proteins were selected on the right panel. (B and C) Venn diagram showed the number of significantly changed proteins and ciliary proteins (CiliaCarta). The gray shaded area represented the overlapping cilia proteins (B). The five overlapped proteins were depicted as a heatmap (green, downregulation; red, upregulation). Note that KIF2A was the most upregulated cilia protein in RGS12 KO groups (C). (D) The synovial fibroblasts were harvested as described in Figure 3A. KIF2A expression levels were measured by western blot. Note that RGS12 KO promotes KIF2A expression, whereas the RGS12 OE inhibits KIF2A expression in synovial fibroblasts (n = 5; ***$p < 0.001$). (E) The synovial fibroblasts were stably transfected with pCMV-vector (control [Ctrl]) or pCMV-RGS12 (RGS12 OE) plasmids. The cell lysates were incubated with anti-Ub or control immunoglobulin G (IgG) antibodies, and bound protein was examined by immunoblotting as indicated. The relative levels of bound KIF2A and Ub proteins were measured by immunoblotting. The values are the mean ± standard error of the mean (n = 5; ***$p < 0.001$). (F and G) The synovial fibroblasts were transfected with pCMV-RGS12 (RGS12 OE) and pCMV-KIF2A (KIF2A OE) or pCMV-Vector (Ctrl) for 48 h. Primary cilia were visualized by immunofluorescence labeling of Ac-Tubulin and ARL13b (scale bar, 10 μm). Note that KIF2A OE can inhibit the increased ciliogenesis caused by RGS12 OE (n = 10; ***$p < 0.001$).

of various pattern recognition receptors that can detect invading pathogens and joint damage.[28,31] However, the specific mechanism of synovial fibroblast activation remains unclear. In this study, we identified the critical role of RGS12-mediated primary cilia in the migratory, adhesive, and secretory properties of synovial fibroblasts during the pathogenesis of arthritis.

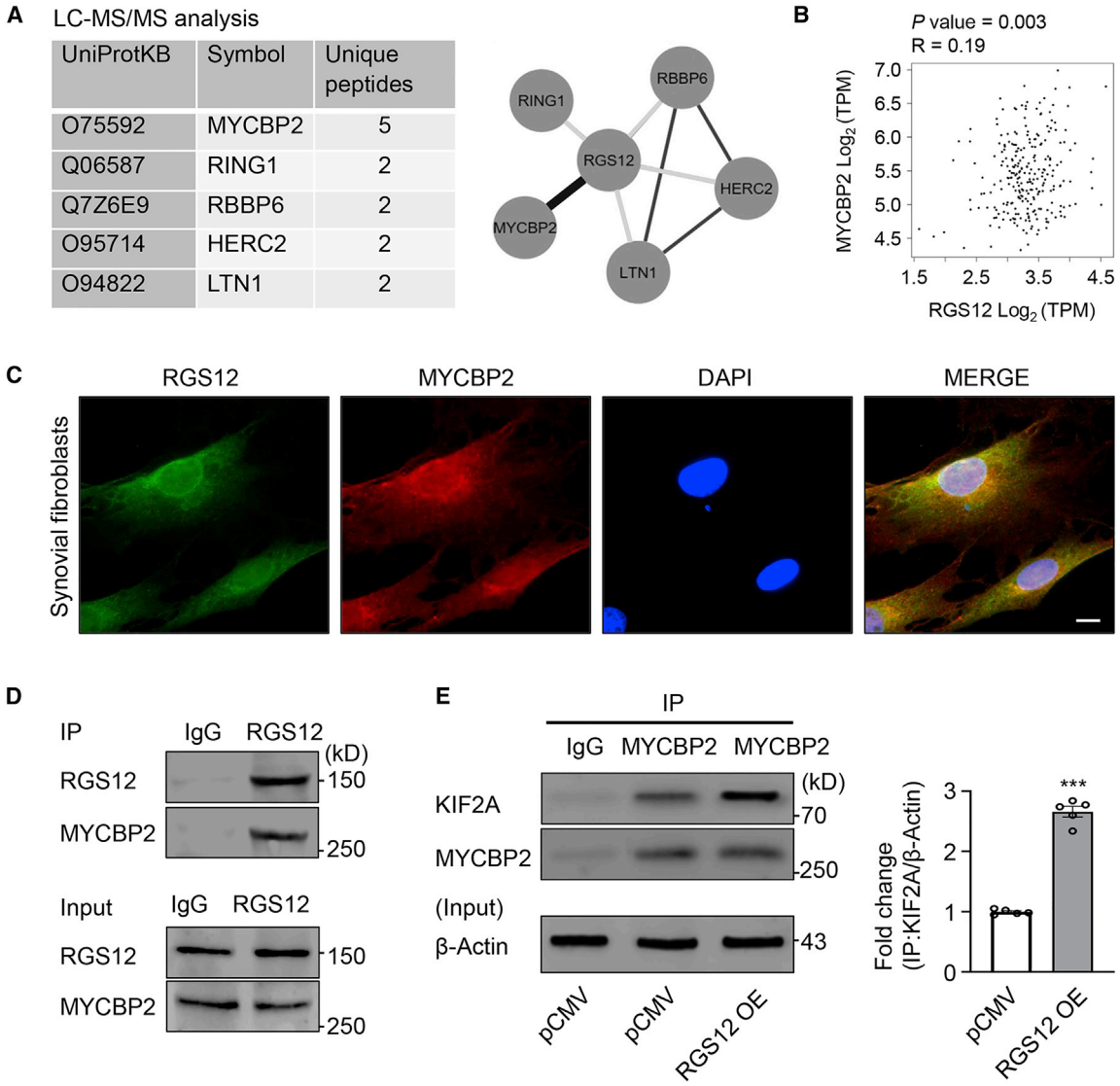

Figure 5. RGS12 promotes the degradation of KIF2A by enhancing the association of KIF2A-MYCBP2

(A) HEK293T cells were stabled transfected with pCMV-Flag or pCMV-RGS12-Flag plasmids. The cell lysates were incubated with the anti-Flag antibody, and the bound protein was examined by LC-MS/MS analysis. The Ub-related proteins were indicated in the left table. The module of the RGS12-Ub-related protein network was shown on the right. Nodes represented proteins, and edges showed the interactions identified by LC-MS and STRING database. The widths of the edges were proportional to the number of unique peptide cross-links. (B) Pearson's correlation analysis of RGS12 and MYCBP2 was analyzed by GEPIA in fibroblasts. (C) Immunofluorescence indicating that RGS12 and MYCBP2 show colocalization in synovial fibroblasts (scale bar, 10 μm). (D) RGS12 interacts with MYCBP2 in synovial fibroblasts (co-immunoprecipitation [IP] assay). The cell lysates were incubated with anti-RGS12 or control immunoglobulin G (IgG) antibodies and bound MYCBP2 was examined by western blot. (E) Synovial fibroblasts were stably transfected with pCMV or pCMV-RGS12 plasmids. The cell lysates were incubated with anti-MYCBP2 or control IgG antibody, and bound KIF2A was examined by western blot. The statistical data showed the relative expression of bound KIF2A (right). Note that RGS12 OE enhanced the combination of MYCBP2 and KIF2A ($n = 5$; ***$p < 0.001$).

Primary cilia are related to a number of pathological conditions.[9,32] In this study, we found that more cilia are produced and elongated in synovial fibroblasts during inflammatory arthritis, which suggests that ciliogenesis is positively related to the development of arthritis. Supportively, the degenerative condition of osteoarthritis is associated with increased expression of cilium-related hedgehog signaling genes.[33] The cilium-related proteins C5orf30 and GSN were demonstrated to be negative regulators of arthritis in mice.[34,35] The ciliary protein SPAG16 in synovial fibroblasts was reported to be a genetic risk factor for joint damage progression in patients with rheumatoid arthritis.[36] The primary cilium acts as a hub for several cell signaling pathways, including the Notch and WNT pathways.[37,38] Thus, the

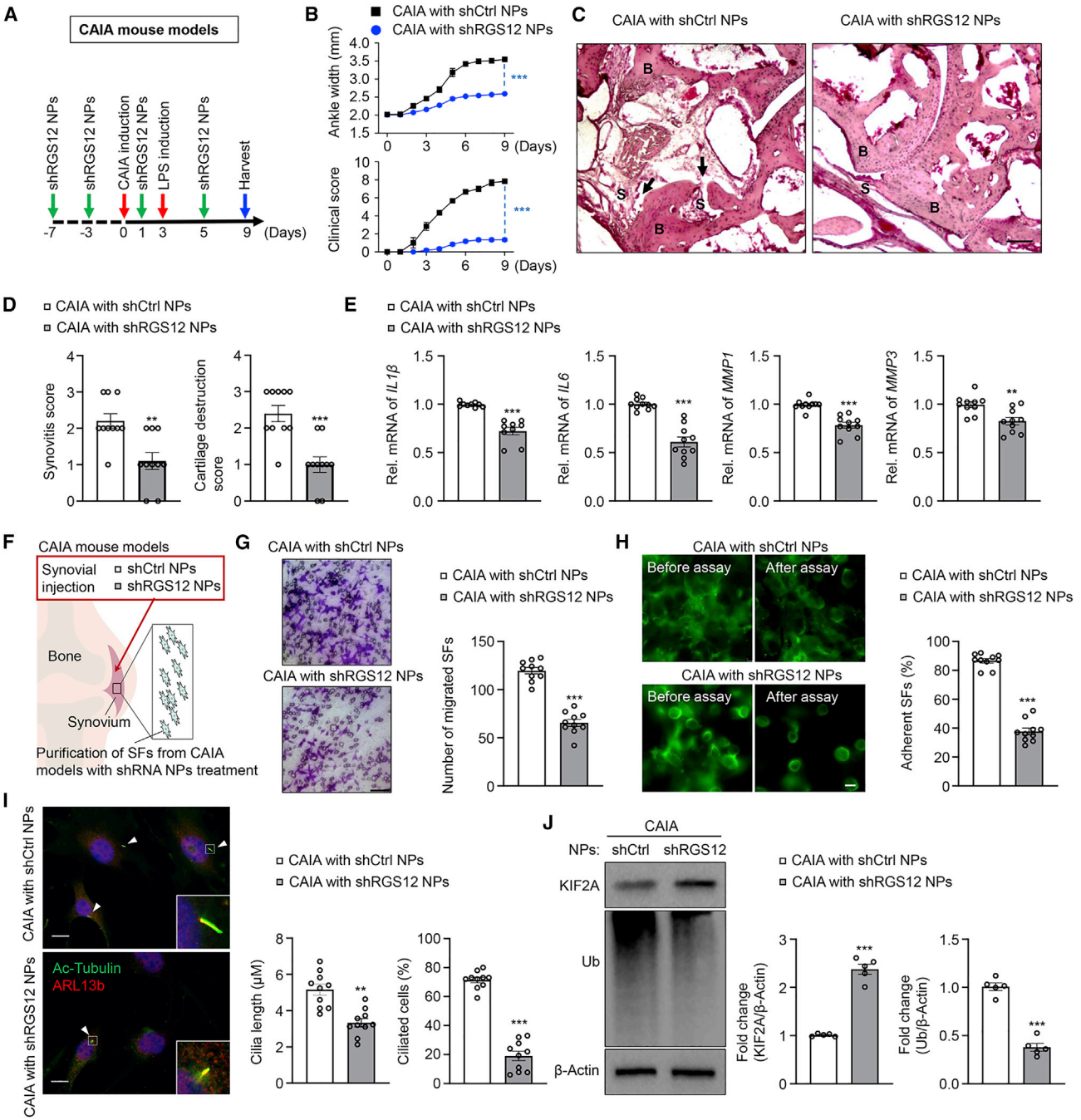

Figure 6. Synovial injection of shRGS12 NPs inhibits the progression of inflammatory arthritis by decreasing ciliogenesis and synovial fibroblast activity

(A) Graphical representation of the experimental strategy. shRGS12 or shCtrl NPs (10 μg) were injected through the synovial cavity 7 days before the CAIA induction (twice per week). CAIA mouse models were induced in C57BL/6 mice by injecting 5 mg of mAb mixture (Chondrex #53100) suspended in sterile PBS and subsequent challenge with 50 μg lipopolysaccharide on day 3. At 9 days after immunization, the mice were sacrificed. (B) Ankle widths and clinical scores of CAIA mice with shCtrl or shRGS12 NPs treatment were evaluated for 9 days. The values are the mean ± standard error of the mean (n = 5; ***p < 0.001). (C) Hematoxylin and eosin staining showed a decrease of inflamed synovium in the CAIA mice with shRGS12 NPs treatment. B, bone area; S, synovium (scale bar, 200 μm). (D) Synovitis score and cartilage destruction score were evaluated from (C). The data were expressed as the means ± standard error of the mean (n = 10; **p < 0.01; ***p < 0.001). (E) Real-time PCR analysis for the expression of *IL1β*, *IL6*, *MMP1*, and *MMP3* in synovium from the CAIA mice with shCtrl NPs and shRGS12 NPs treatments (n = 10; **p < 0.01; ***p < 0.001). (F) The sketch showing that the

(legend continued on next page)

increased ciliogenesis in synovial fibroblasts during arthritis may enhance the transduction of inflammatory signals to regulate cellular functions.

RGS12 contains several functional domains that regulate multiple signaling pathways.[39,40] We previously found that RGS12 enhances the SUMOylation and phosphorylation of the PTEN protein.[19] Ub-proteasome-mediated degradation is essential for the regulation of a number of cellular processes, such as ciliogenesis, and defects in cilia contribute to a number of disorders ranging from the development of cystic kidneys to perturbed left-right symmetry.[41–43] In this study, we found that RGS12 enhanced Ub levels by activating the Ub ligase MYCBP2 and, therefore, degraded the KIF2A protein. KIF2A is a ciliary protein that localizes to mitotic spindle microtubules and poles to promote primary cilia disassembly via microtubule depolymerization.[12] Loss of KIF2A in hTERT-RPE1 KO cells caused impairment of primary cilia disassembly after inappropriate ciliogenesis.[12] We found that the KIF2A level was quantitatively controlled by the Ub ligase MYCBP2 and that RGS12 was associated with MYCBP2, but not with KIF2A in synovial fibroblasts. Thus, our findings suggest that RGS12 may serve as a scaffold that binds to MYCBP2 to promote the degradation of KIF2A.

In summary, this study provides the first evidence that RGS12 promotes ciliogenesis by regulating KIF2A stability in inflammatory arthritis (Figure 7). The increased ciliogenesis results in the activation of synovial fibroblasts, which leads to joint swelling and cartilage damage. Therefore, this study provides genetic evidence that RGS12 may be a potential drug target for the treatment of inflammatory arthritis.

MATERIALS AND METHODS

Cre/flox mouse generation

To generate RGS12-KO mice, RGS12$^{fl/fl}$ mice were crossed with mice expressing Cre recombinase under the control of the tamoxifen-inducible chicken beta actin promoter/enhancer fused to the cytomegalovirus promoter (B6.Cg-Tg (CAG-Cre/Esr1*) 5Amc/J or CAG-CreER; Stock No: 004,682, The Jackson Laboratory). Recipient mice were injected intraperitoneally with 100 mg/kg body weight tamoxifen daily for 5 consecutive days.[44] CAG-CreER control and (CAG-CreER; RGS12$^{fl/fl}$) KO mice (8 weeks old; n = 20) were littermates derived from breeding heterozygous animals. Mice were fed a chow diet and raised in a clean room on a 12-h light/12-h dark cycle. All animal studies were performed in accordance with institutional guidelines and with approval by the Institutional Animal Care and Use Committee of the University of Pennsylvania.

CAIA mouse models

CAIA was induced in control and RGS12 KO mice (C57BL/6 background; 8 weeks old; n = 10) using a mixture of 5 mg of mAbs (Chondrex #53100) according to the manufacturer's instructions. Mice in both groups were intraperitoneally injected with 5 mg of mAbs on day 0 and 50 μg lipopolysaccharide (Chondrex #9028) on day 3 to synchronize the development of arthritis.[45] Mice began to develop arthritis on day 4 and were euthanized with carbon dioxide on day 9.

Clinical scoring of CAIA in the model

Each hind paw of the mice was scored on a scale of 0–3 based on the following evaluation criteria: 0 (normal), 1 (emergence of ankle swelling), 2 (moderate to severe redness and swelling of the ankle, wrist, and pad), and 3 (swelling of the entire paw, including digits, and inflamed limbs with involvement of multiple joints).[46] The thickness of each hind paw was measured using a thickness gauge and is expressed in millimeters.

Synovial injection of shRGS12 NPs in CAIA mice

shRGS12 or shCtrl NPs were injected through the synovial cavity 7 days before the CAIA induction (twice per week). For each injection, 10 μg of psi-nU6.1-shRGS12 was mixed with 20 μL of a NP *in vivo* DNA transfection reagent (Entranster *in vivo*; North Shore) according to the manufacturer's protocol and the procedure previously described.[47] Mice synovial tissues were harvested on day 9.

Histological scoring

Hind paws were fixed in 10% formalin, decalcified, and embedded in paraffin. Tissues were sliced into 6-μm sections and stained with hematoxylin and eosin to assess joint pathology. The degrees of cartilage damage and inflammation in the joints were determined using standard scoring.[48] The severity of inflammation was scored according to the extent of inflammatory cell infiltration into the infrapatellar fat pads, joint capsule, and area adjacent to the periosteal sheath (0, absent; 1, mild [1%–10%]; 2, moderate [11%–50%]; or 3, severe [51%–100%]). Cartilage destruction was scored according to the percentage of the cartilage surface that was eroded (0, absent; 1, mild [1%–10%]; 2, moderate [11%–50%]; or 3, severe [51%–100%]).[48,49]

Cell culture

Primary synovial fibroblasts were isolated from knee and ankle synovium of CAG-CreER control and RGS12 KO mice with or without CAIA as described.[50] In brief, synovial tissues were minced and dissociated prior to gentle rocking for 2 h at 37°C in DMEM (Sigma-Aldrich) containing 1 mg/mL type IV collagenase (Worthington Biochemical) and 0.1 mg/mL DNase (Sigma-Aldrich).

primary synovial fibroblasts (SFs) purified from the CAIA mouse models were treated with shCtrl and shRGS12 NPs, respectively. (G) The migration of SFs from CAIA mice was inhibited by the shRGS12 NPs treatment (n = 10; ***p < 0.001; scale bar, 200 μm). (H) The attachment of SFs from CAIA mice was repressed by the treatment of shRGS12 NPs (scale bar, 10 μm). The data are presented as the mean ± standard error of the mean (n = 10; ***p < 0.001). (I) The lengths of cilia and the ciliated cell numbers in synovial fibroblasts were decreased in shRGS12 NPs treatment (n = 10; **p < 0.01; ***p < 0.001; scale bar, 10 μm). (J) The synovial fibroblasts were harvested as described in (F). The protein expression levels of KIF2A, Ub, and β-actin were determined by Western blot. Note that shRGS12 NPs promote KIF2A expression whereas inhibit the Ub expression. The data are presented as the mean ± standard error of the mean (n = 5; ***p < 0.001).

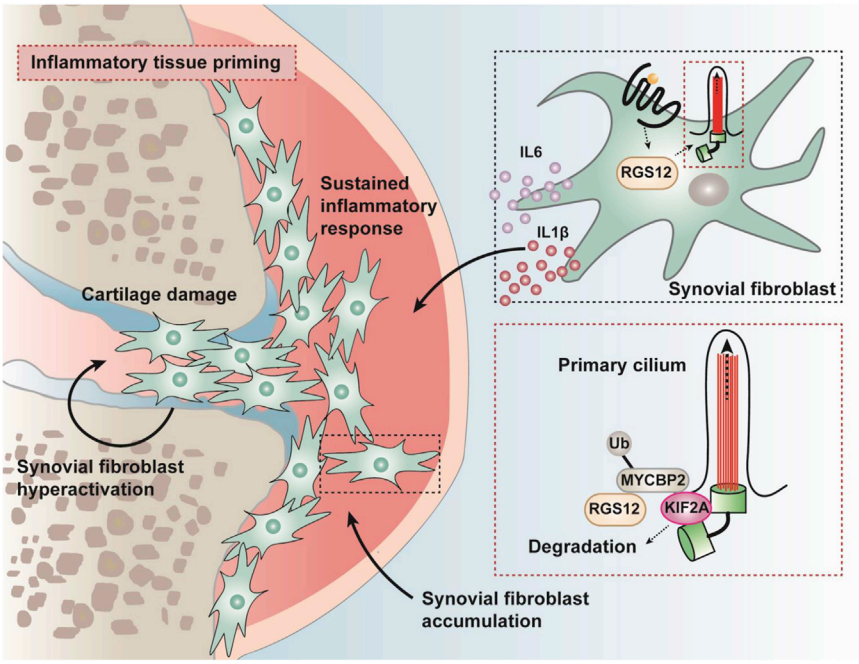

Figure 7. Schematic for RGS12 in synovial fibroblasts regulates the inflammatory arthritis

Inflammatory signals enhance RGS12 expression in synovial fibroblasts, which leads to synovial fibroblast accumulation, hyperactivation, and a sustained inflammatory response. Mechanism studies showed the upregulation of RGS12 promotes ciliogenesis by activating MYCBP2-mediated degradation of KIF2A. The increased ciliogenesis leads to the enhancement of synovial fibroblast migration, attachment, and secretion in the synovium, which thereby contributes to joint swelling and cartilage damage.

The isolated fibroblasts were suspended in PBS containing an anti-CD90 antibody (Proteintech, 66766-1-Ig) for 30 min and were then washed with PBS and mixed with streptavidin-labeled magnetic beads (Thermo Fisher Scientific,11203D). Labeled cells were subjected to magnetic separation and collected by the addition of DMEM. Fibroblasts were cultured in DMEM/F12 (Thermo Fisher Scientific) supplemented with 10% fetal bovine serum (FBS), nonessential amino acids, sodium pyruvate, and 1% penicillin/streptomycin (Thermo Fisher Scientific). Cultures were serum starved for 12 h to promote ciliogenesis. The SW982 human synovial cell line (HTB-93; ATCC) was maintained in Leibovitz's L-15 medium supplemented with 2 mM glutamine, 100 U/mL penicillin, 100 mg/mL streptomycin, and 10% FBS. The ADTC mouse chondrocyte cell line (99,072,806; Sigma-Aldrich) or C20A4 human chondrocyte cell line (SCC041, Sigma-Aldrich) were maintained in DMEM/F12 supplemented with 2 mM glutamine, 100 U/mL penicillin, 100 mg/mL streptomycin, and 5% FBS.

Immunofluorescence

Primary synovial fibroblasts or SW982 cells were fixed with 4% paraformaldehyde for 10 min at room temperature and incubated with an anti-acetylated α-tubulin (1:100 dilution; Sigma-Aldrich), anti-RGS12 (1:100 dilution; Sigma-Aldrich), anti-KIF2A (1:200 dilution; Proteintech, or anti-MYCBP2 (1:100 dilution; Sigma-Aldrich) antibody before incubation with the appropriate secondary antibody (1:500 dilution; Jackson ImmunoResearch Laboratory). A LAS-X (Leica) microscope was used to create maximum projections of z-stacks from which the cilia length and ciliated cell numbers were measured using ImageJ software (National Institutes of Health).[9] At least three different mounted preparations were used to acquire images of cells in five fields of view per subgroup at 40× magnification. All images were visualized on a microscope and acquired with the same exposure time. The relative fluorescence intensity values were determined by comparing each intensity value with the average intensity over the field of view.

Cell adhesion assay

For the plastic adhesion assay, synovial fibroblasts were centrifuged and seeded in 24-well plates at 1×10^4 cells/well. After incubation for 12 h at 37°C, the plates were shaken at full speed for 5 min, and nonadherent or weakly attached cells were removed by washing with PBS. The remaining attached synovial fibroblasts were stained with 0.1% crystal violet dye in methanol for 10 min and counted under a microscope.

Flipping assay

For the cell-cell binding assay, ADTC5 or C20A4 chondrocytes were seeded in 24-well plates and cultured to 100% confluence. Synovial fibroblasts were stably transfected with pCMV-GFP plasmids, and the same number of GFP-labeled synovial fibroblasts was then plated on top of the monolayer and allowed to attach for 2 h (before assay). The dish was flipped 180° and shaken, and the number of GFP-labeled synovial fibroblasts remaining on the substrate was counted (after assay). The ratio of the total area of fluorescence in the post-flipping image to that in the pre-flipping image was calculated to determine the percentage of cells that remained attached.[51]

Migration assay

The fibroblast migration assay was performed using the Boyden chamber method and 6.5-mm diameter filters with an 8.0-mm pore size (Corning). Briefly, synovial fibroblasts were seeded into a Boyden chamber at a final concentration of 6×10^4 cells/mL. DMEM/F12 was added to the upper compartments, and DMEM/F12 supplemented with 10% FBS was added to the lower compartments. The chambers were incubated at 37°C in the presence of 5% CO_2 for 24 h. Cells on the filters were fixed with methanol for 15 min and stained with 0.1% crystal violet for 15 min. Migration was quantified by counting the stained cells that migrated to the lower side of the filter. The mean number of stained cells per 10 random fields of view was counted for each assay.

WST-1 assay

The cell proliferation and viability assay was performed by following the WST-1 kit instructions (Sigma-Aldrich). Briefly, synovial fibroblasts were seeded in 90 μL fresh growth medium supplemented with 10 μL of WST-1 reagent and were then incubated at 37°C for 1 h. The absorbance was measured at 490 nm using a 96-well plate reader (Bio-Rad).

Plasmid construction

Mouse RGS12 (NM_173402.2) cDNA was cloned and inserted into the p3xFLAG-Myc-CMV-26 backbone (Sigma-Aldrich). The nontargeting RGS12 short hairpin/small interfering RNA (sh/siRNA) and RGS12 sh/siRNAs were obtained from GeneCopoeia. Target sequences were as follows: control sh/siRNA: GCTTCGCGCCGTAGTCTTA; RGS12 sh/siRNA 1: CTAGGCAAGTCTAACTCTATT; RGS12 sh/siRNA 2: CCTGTCCATGATTAATAAAGG; RGS12 sh/siRNA 3: AGTCTGCAACTGTGTCTGATGGCGAGTTG. The pEGFP-KIF2A plasmid was obtained from Addgene (52,401). KIF2A shRNAs were obtained from Santa Cruz Biotechnology (sc-60885-SH).

Cell transfection

Primary synovial fibroblasts isolated from C57/BL6 mice were seeded on six-well plates at 3×10^5 cells/well (approximately 90% confluence). Cells (primary mouse synovial fibroblasts or SW982 cells [HTB-93 – ATCC]) were transfected with pCMV-vector or pCMV-RGS12 or with shControl, shRGS12, or shKIF2A on the following day with Lipofectamine 3000 reagent (Thermo Fisher Scientific) according to the instructions. Cells were harvested 24–48 h after transfection. For stable transfection, synovial fibroblasts were seeded at 2×10^6 cells per well in a six-well plate and transfected with pCMV-vector or pCMV-RGS12 plasmids using Lipo3000 reagent (Thermo Fisher Scientific) according to the manufacturer's instructions. Forty-eight hours after transfection, cells were treated with 0.4 mg/mL geneticin (G418; Thermo Fisher Scientific) every other day for 1 week until G418-resistant colonies had formed. Stably transfected cells were thereafter maintained in complete medium (DMEM supplemented with 2 mM glutamine, 100 U/mL penicillin, 100 mg/mL streptomycin, and 10% FBS) containing 0.4 mg/mL G418.

ELISA

SF lysates were prepared according to the commercial kit instructions (DY401–05, R&D Systems). Standard ELISA kits were used to measure IL6 (KE10007, Proteintech) and IL-1β (DY401-05; R&D Systems) concentrations. The optical density (OD) values of the plate wells were measured at 450 nm, and the OD values for the duplicate wells were averaged.

Western blot analysis

Synovium tissue or synovial fibroblasts were homogenized with radioimmunoprecipitation assay buffer containing protease inhibitor cocktails (PICs) and phenylmethanesulfonylfluoride (phenylmethylsulfonyl fluoride [PMSF]) (Sigma-Aldrich) on ice. Equal amounts of protein (30 μg) from the different groups were denatured in SDS loading buffer and separated on 10% SDS-PAGE gels. Proteins were transferred to NC membranes in the transfer buffer containing 20% methanol. Membranes were sequentially blocked with 5% skim milk, incubated with the primary antibodies described below overnight (4°C), and incubated with horseradish peroxidase (HRP)-conjugated secondary antibody (1:2,000, Jackson ImmunoResearch) at room temperature for 1 h. Signals were analyzed using an enhanced chemiluminescence western blot system (Bio-Rad Laboratories). β-Actin (1:3000, sc-47778 HRP; Santa Cruz) was used as the internal control. The following antibodies were used: anti-RGS12 (1:1,000; GW21317; Sigma-Aldrich), anti-KIF2A (1:1,000; 13105-1-AP; Proteintech), and anti-MYCBP2 (1:1,000; MABN2397; Sigma-Aldrich).

Immunoprecipitation

Primary synovial fibroblasts or HEK293 cells (CRL-1573; ATCC) were lysed in NP-40 buffer supplemented with a PIC and PMSF (Sigma-Aldrich). Briefly, lysates with equal amounts of protein (800 μg) were incubated first with primary antibodies or IgG at room temperature for 1 h and then with protein A/G beads overnight, after which the beads were washed with PBS with Tween. Bound proteins were solubilized in loading buffer for western blot analysis.

LC-MS

LC-MS was performed to compare the protein profiles of bone marrow cells from 8-week-old control and RGS12 KO mice. A stringent set of criteria including a low peptide/protein false discovery rate of less than 0.05 was used for protein identification. Heatmap visualization was performed using the R package cluster. Reactome database (https://reactome.org/) was used to perform gene functional analysis.

Protein-protein interaction analysis

The STRING (https://string-db.org) database was used to predict functional interactions among RGS12 binding proteins. Active interaction sources along with the criterion of an interaction score of more than 0.4, were applied to construct the protein-protein interaction networks. In the networks, the nodes correspond with proteins and the edges represent interactions.

Gene correlation analysis

The GEPIA (http://gepia.cancer-pku.cn/index.html) database was used to confirm the significantly correlated genes in fibroblasts. GEPIA is an interactive database that analyzes RNA sequencing data from the TCGA and GTEx projects. Gene expression correlation analysis was performed on given sets of TCGA expression data. Spearman correlation analysis was used to calculate correlation coefficients. RGS12 is shown on the *x* axis, and other genes of interest are shown on the *y* axis. Pearson correlation coefficients were calculated by using the transformed fibroblast datasets (GTEx).

Real-time PCR

RNA from synovial fibroblasts was isolated using TRIzol reagent (Sigma-Aldrich) according to the manufacturer's instructions. Then, 1 μg of RNA was reverse transcribed into cDNA using a

Reverse Transcription Kit (Takara). Real-time PCR was performed with a reaction mixture containing primers, the cDNA template, and SYBR Green PCR Master Mix (Bimake). The sequences of the real-time PCR primers are listed in Table S3.

Statistical analyses

All data are expressed as the mean ± standard error of the mean. Statistical significance was determined by unpaired two-tailed Student's t-test. Analysis of variance was first performed to compare the mean values among groups, and the Student-Newman-Keuls test was used to compare the mean values between two conditions with GraphPad software 7.0 (San Diego). A p values of less than 0.05 was considered significant.

DATA AVAILABILITY

The authors declare that all data supporting the findings of this study are available within the paper and its supplemental information files.

SUPPLEMENTAL INFORMATION

Supplemental information can be found online at https://doi.org/10.1016/j.omtn.2022.12.017.

ACKNOWLEDGMENTS

The authors thank Dr. Yan Yan from the tissue processing core at the School of Dental Medicine (University of Pennsylvania) for her specialized histological support. We thank Dr. Andrew Ng (State University of New York at Buffalo) for his help with LC-MS data collection. This work was supported by grants from the National Institute on Aging [NIA] (AG048388), the National Institute of Arthritis and Musculoskeletal and Skin Diseases [NIAMS] (AR066101), and the Congressionally Directed Medical Research Programs [CDMRP] (PR201467) to S.Y. This work was also supported by grants from the Penn Center for Musculoskeletal Disorders (PCMD), [NIAMS] P30-AR069619.

AUTHOR CONTRIBUTIONS

Study design: S.Y. and G.Y.; sample collection: G.Y. and St.Y.; experiments and data analysis: G.Y. and S.Y.; data interpretation: G.Y. and S.Y.; writing of the manuscript: G.Y. and S.Y.; critical proofreading of the manuscript: all authors.

DECLARATION OF INTERESTS

The authors declare no competing interests.

REFERENCES

1. Lefèvre, S., Knedla, A., Tennie, C., Kampmann, A., Wunrau, C., Dinser, R., Korb, A., Schnäker, E.M., Tarner, I.H., Robbins, P.D., et al. (2009). Synovial fibroblasts spread rheumatoid arthritis to unaffected joints. Nat. Med. *15*, 1414–1420.
2. Gravallese, E.M. (2002). Bone destruction in arthritis. Ann. Rheum. Dis. *61*, 84–86.
3. Pap, T., Meinecke, I., Müller-Ladner, U., and Gay, S. (2005). Are fibroblasts involved in joint destruction? Ann. Rheum. Dis. *64*, 52–54.
4. Croft, A.P., Campos, J., Jansen, K., Turner, J.D., Marshall, J., Attar, M., Savary, L., Wehmeyer, C., Naylor, A.J., Kemble, S., et al. (2019). Distinct fibroblast subsets drive inflammation and damage in arthritis. Nature *570*, 246–251.
5. Müller-Ladner, U., Pap, T., Gay, R.E., Neidhart, M., and Gay, S. (2005). Mechanisms of disease: the molecular and cellular basis of joint destruction in rheumatoid arthritis. Nat. Clin. Pract. Rheumatol. *1*, 102–110.
6. Pap, T., Müller-Ladner, U., Gay, R.E., and Gay, S. (2000). Fibroblast biology. Role of synovial fibroblasts in the pathogenesis of rheumatoid arthritis. Arthritis Res. *2*, 361–367.
7. Buckley, C.D., Pilling, D., Lord, J.M., Akbar, A.N., Scheel-Toellner, D., and Salmon, M. (2001). Fibroblasts regulate the switch from acute resolving to chronic persistent inflammation. Trends Immunol. *22*, 199–204.
8. Rattner, J.B., Sciore, P., Ou, Y., van der Hoorn, F.A., and Lo, I.K.Y. (2010). Primary cilia in fibroblast-like type B synoviocytes lie within a cilium pit: a site of endocytosis. Histol. Histopathol. *25*, 865–875.
9. Wann, A.K.T., and Knight, M.M. (2012). Primary cilia elongation in response to interleukin-1 mediates the inflammatory response. Cell. Mol. Life Sci. *69*, 2967–2977.
10. Goetz, S.C., and Anderson, K.V. (2010). The primary cilium: a signalling centre during vertebrate development. Nat. Rev. Genet. *11*, 331–344.
11. Hildebrandt, F., Benzing, T., and Katsanis, N. (2011). Ciliopathies. N. Engl. J. Med. *364*, 1533–1543.
12. Miyamoto, T., Hosoba, K., Ochiai, H., Royba, E., Izumi, H., Sakuma, T., Yamamoto, T., Dynlacht, B.D., and Matsuura, S. (2015). The microtubule-depolymerizing activity of a mitotic kinesin protein KIF2A drives primary cilia disassembly coupled with cell proliferation. Cell Rep. *10*, 664–673.
13. Wann, A.K.T., Chapple, J.P., and Knight, M.M. (2014). The primary cilium influences interleukin-1beta-induced NFkappaB signalling by regulating IKK activity. Cell. Signal. *26*, 1735–1742.
14. Kehrl, J.H. (1998). Heterotrimeric G protein signaling: roles in immune function and fine-tuning by RGS proteins. Immunity *8*, 1–10.
15. Patel, J., McNeill, E., Douglas, G., Hale, A.B., de Bono, J., Lee, R., Iqbal, A.J., Regan-Komito, D., Stylianou, E., Greaves, D.R., and Channon, K.M. (2015). RGS1 regulates myeloid cell accumulation in atherosclerosis and aortic aneurysm rupture through altered chemokine signalling. Nat. Commun. *6*, 6614.
16. Kimple, A.J., Garland, A.L., Cohen, S.P., Setola, V., Willard, F.S., Zielinski, T., Lowery, R.G., Tarran, R., and Siderovski, D.P. (2014). RGS21, a regulator of taste and mucociliary clearance? Laryngoscope *124*, E56–E63.
17. Louwette, S., Labarque, V., Wittevrongel, C., Thys, C., Metz, J., Gijsbers, R., Debyser, Z., Arnout, J., Van Geet, C., and Freson, K. (2012). Regulator of G-protein signaling 18 controls megakaryopoiesis and the cilia-mediated vertebrate mechanosensory system. FASEB J *26*, 2125–2136.
18. Yuan, G., Yang, S., Liu, M., and Yang, S. (2020). RGS12 is required for the maintenance of mitochondrial function during skeletal development. Cell Discov. *6*, 59.
19. Fu, C., Yuan, G., Yang, S.T., Zhang, D., and Yang, S. (2021). RGS12 represses oral cancer via the phosphorylation and SUMOylation of PTEN. J. Dent. Res. *100*, 522–531.
20. Kim, J., Lee, J.E., Heynen-Genel, S., Suyama, E., Ono, K., Lee, K., Ideker, T., Aza-Blanc, P., and Gleeson, J.G. (2010). Functional genomic screen for modulators of ciliogenesis and cilium length. Nature *464*, 1048–1051.
21. Veland, I.R., Lindbæk, L., and Christensen, S.T. (2014). Linking the primary cilium to cell migration in tissue repair and brain development. Bioscience *64*, 1115–1125.
22. Seeger-Nukpezah, T., and Golemis, E.A. (2012). The extracellular matrix and ciliary signaling. Curr. Opin. Cell Biol. *24*, 652–661.
23. Stanford, S.M., Aleman Muench, G.R., Bartok, B., Sacchetti, C., Kiosses, W.B., Sharma, J., Maestre, M.F., Bottini, M., Mustelin, T., Boyle, D.L., et al. (2016). TGFbeta responsive tyrosine phosphatase promotes rheumatoid synovial fibroblast invasiveness. Ann. Rheum. Dis. *75*, 295–302.
24. Opalenik, S.R., and Davidson, J.M. (2005). Fibroblast differentiation of bone marrow-derived cells during wound repair. FASEB J *19*, 1561–1563.
25. Ichim, T.E., O'Heeron, P., and Kesari, S. (2018). Fibroblasts as a practical alternative to mesenchymal stem cells. J. Transl. Med. *16*, 212.
26. van Dam, T.J.P., Kennedy, J., van der Lee, R., de Vrieze, E., Wunderlich, K.A., Rix, S., Dougherty, G.W., Lambacher, N.J., Li, C., Jensen, V.L., et al. (2019). CiliaCarta: an integrated and validated compendium of ciliary genes. PLoS One *14*, e0216705.

27. Neumann, E., Lefèvre, S., Zimmermann, B., Gay, S., and Müller-Ladner, U. (2010). Rheumatoid arthritis progression mediated by activated synovial fibroblasts. Trends Mol. Med. *16*, 458–468.

28. Nygaard, G., and Firestein, G.S. (2020). Restoring synovial homeostasis in rheumatoid arthritis by targeting fibroblast-like synoviocytes. Nat. Rev. Rheumatol. *16*, 316–333.

29. Bartok, B., and Firestein, G.S. (2010). Fibroblast-like synoviocytes: key effector cells in rheumatoid arthritis. Immunol. Rev. *233*, 233–255.

30. Edwards, J.C. (1995). Synovial intimal fibroblasts. Ann. Rheum. Dis. *54*, 395–397.

31. Ospelt, C. (2017). Synovial fibroblasts in 2017. RMD Open *3*, e000471.

32. Dinsmore, C., and Reiter, J.F. (2016). Endothelial primary cilia inhibit atherosclerosis. EMBO Rep. *17*, 156–166.

33. Thompson, C.L., Chapple, J.P., and Knight, M.M. (2014). Primary cilia disassembly down-regulates mechanosensitive hedgehog signalling: a feedback mechanism controlling ADAMTS-5 expression in chondrocytes. Osteoarthritis Cartilage *22*, 490–498.

34. Muthana, M., Hawtree, S., Wilshaw, A., Linehan, E., Roberts, H., Khetan, S., Adeleke, G., Wright, F., Akil, M., Fearon, U., et al. (2015). C5orf30 is a negative regulator of tissue damage in rheumatoid arthritis. Proc. Natl. Acad. Sci. USA *112*, 11618–11623.

35. Aidinis, V., Carninci, P., Armaka, M., Witke, W., Harokopos, V., Pavelka, N., Koczan, D., Argyropoulos, C., Thwin, M.M., Möller, S., et al. (2005). Cytoskeletal rearrangements in synovial fibroblasts as a novel pathophysiological determinant of modeled rheumatoid arthritis. PLoS Genet. *1*, e48.

36. de Rooy, D.P.C., Tsonaka, R., Andersson, M.L.E., Forslind, K., Zhernakova, A., Frank-Bertoncelj, M., de Kovel, C.G.F., Koeleman, B.P.C., van der Heijde, D.M.F.M., Huizinga, T.W.J., et al. (2015). Genetic factors for the severity of ACPA-negative rheumatoid arthritis in 2 cohorts of early disease: a genome-wide study. J. Rheumatol. *42*, 1383–1391.

37. Ezratty, E.J., Stokes, N., Chai, S., Shah, A.S., Williams, S.E., and Fuchs, E. (2011). A role for the primary cilium in Notch signaling and epidermal differentiation during skin development. Cell *145*, 1129–1141.

38. Pala, R., Alomari, N., and Nauli, S.M. (2017). Primary cilium-dependent signaling mechanisms. Int. J. Mol. Sci. *18*, 2272.

39. Gross, J.D., Kaski, S.W., Schroer, A.B., Wix, K.A., Siderovski, D.P., and Setola, V. (2018). Regulator of G protein signaling-12 modulates the dopamine transporter in ventral striatum and locomotor responses to psychostimulants. J. Psychopharmacol. *32*, 191–203.

40. Schiff, M.L., Siderovski, D.P., Jordan, J.D., Brothers, G., Snow, B., De Vries, L., Ortiz, D.F., and Diversé-Pierluissi, M. (2000). Tyrosine-kinase-dependent recruitment of RGS12 to the N-type calcium channel. Nature *408*, 723–727.

41. Kasahara, K., Kawakami, Y., Kiyono, T., Yonemura, S., Kawamura, Y., Era, S., Matsuzaki, F., Goshima, N., and Inagaki, M. (2014). Ubiquitin-proteasome system controls ciliogenesis at the initial step of axoneme extension. Nat. Commun. *5*, 5081.

42. Ong, A.C.M., and Wheatley, D.N. (2003). Polycystic kidney disease–the ciliary connection. Lancet *361*, 774–776.

43. Manning, D.K., Sergeev, M., van Heesbeen, R.G., Wong, M.D., Oh, J.H., Liu, Y., Henkelman, R.M., Drummond, I., Shah, J.V., and Beier, D.R. (2013). Loss of the ciliary kinase Nek8 causes left-right asymmetry defects. J. Am. Soc. Nephrol. *24*, 100–112.

44. Wang, G., Liu, X., Gaertig, M.A., Li, S., and Li, X.J. (2016). Ablation of huntingtin in adult neurons is nondeleterious but its depletion in young mice causes acute pancreatitis. Proc. Natl. Acad. Sci. USA *113*, 3359–3364.

45. Danks, L., Komatsu, N., Guerrini, M.M., Sawa, S., Armaka, M., Kollias, G., Nakashima, T., and Takayanagi, H. (2016). RANKL expressed on synovial fibroblasts is primarily responsible for bone erosions during joint inflammation. Ann. Rheum. Dis. *75*, 1187–1195.

46. Crow, A.R., Kapur, R., Koernig, S., Campbell, I.K., Jen, C.C., Mott, P.J., Marjoram, D., Khan, R., Kim, M., Brasseit, J., et al. (2019). Treating murine inflammatory diseases with an anti-erythrocyte antibody. Sci. Transl. Med. *11*, eaau8217.

47. Zheng, X., Cheng, M., Fu, B., Fan, X., Wang, Q., Yu, X., Sun, R., Tian, Z., and Wei, H. (2015). Targeting LUNX inhibits non-small cell lung cancer growth and metastasis. Cancer Res. *75*, 1080–1090.

48. Alabarse, P.V.G., Lora, P.S., Silva, J.M.S., Santo, R.C.E., Freitas, E.C., de Oliveira, M.S., Almeida, A.S., Immig, M., Teixeira, V.O.N., Filippin, L.I., and Xavier, R.M. (2018). Collagen-induced arthritis as an animal model of rheumatoid cachexia. J. Cachexia Sarcopenia Muscle *9*, 603–612.

49. Armaka, M., Ospelt, C., Pasparakis, M., and Kollias, G. (2018). The p55TNFR-IKK2-Ripk3 axis orchestrates arthritis by regulating death and inflammatory pathways in synovial fibroblasts. Nat. Commun. *9*, 618.

50. Zhao, J., Ouyang, Q., Hu, Z., Huang, Q., Wu, J., Wang, R., and Yang, M. (2016). A protocol for the culture and isolation of murine synovial fibroblasts. Biomed. Rep. *5*, 171–175.

51. Roycroft, A., Szabó, A., Bahm, I., Daly, L., Charras, G., Parsons, M., and Mayor, R. (2018). Redistribution of adhesive forces through Src/FAK drives contact inhibition of locomotion in neural crest. Dev. Cell *45*, 565–579.e3.